

**An Observational Study of Summertime Ice Formation
at the Ice Valley in Milyang, Korea**

By

H.L. TANAKA, Sung-Euii MOON, and Soo-Jin HWANG

*Reprinted from the Science Reports of
the Institute of Geoscience, University of Tsukuba
Section A, Volume 20, pp. 33-51
January 25, 1999*

An Observational Study of Summertime Ice Formation at the Ice Valley in Milyang, Korea

By

H.L. TANAKA, Sung-Euii MOON*, and Soo-Jin HWANG†

Contents

1. Introduction	34
2. Description of the Ice Valley	35
3. Observation items and method	37
4. Result of the observation	39
5. Summary and discussion	49
Acknowledgments	50

Abstract

The Ice Valley's ice freezes during spring to summer and it disappears during fall to winter. It has been said that the hotter the summer is, the more the summertime ice grows. In this study, we have conducted *in situ* observation of Ice Valley in Milyang, Korea during June 3 to 5, 1997 as a collaborative study between the University of Tsukuba, Japan and the Pusan National University, Korea.

The result of the observation shows following facts: 1) The blowing air temperature in the wind caves is 0°C near the freezing area around the 410 m point above the sea level along the Ice Valley. We find that there is no diurnal variation in temperature where cold air blows out from the wind cave for the altitudes from 360 to 430 m along the slope. 2) Cold air blowing from the wind caves at the freezing area merges in one to produce cold air drainage (katabatic wind). It is confined within 5 m height above the ground at the freezing area. Beyond that level, ordinary valley wind (anabatic wind) is observed. 3) The vertical sounding at 410 m point along the slope shows that the upper air temperature over the valley is 24°C and humidity 25% in average. Within the thin layer from the surface to 5 m above the ground, the temperature decreases rapidly from 24°C to 0°C at the ice location in the wind cave. Likewise, the humidity increases from 25% to 100% within the thin layer.

It is shown from the result that the surface cold air drainage (katabatic wind) and the upper air valley wind (anabatic wind) are the separated wind system with no continuity. The result of present observation supports the theory of the selective convection during winter and summer as a thermal filter for the ice formation. However, the detail of the mysterious behavior of Ice Valley's ice remains unveiled.

* Korea Meteorological Administration

† Pusan National University

1. Introduction

Ice Valley at Milyang, Korea is a famous summer resort in that natural ice freezes during hot season from early April to late August along a mountain slope. The cool and beautiful valley attracts many tourists who wish to see the Ice Valley's ice. Recently, a modern style gorgeous hotel is built at the entrance area of the Natural Monument of the Ice Valley to attract more tourists to see the mysterious summertime ice.

The Ice Valley's ice appears during spring to summer and it disappears during fall to winter. Surprisingly, it has been said that the hotter the summer is, the more the amount of summertime ice is. On the contrary, the ice tends to shrink when, for example, the summer is cooler due to the prolonged Baitu season. The ice partially melts after the rainfall due to the warmth of rain, but it freezes a few days after again. In the rainy season, which starts in early August, the ice completely melts due to the heavy and continuous rain. However, in the event of a short rainy season or if the weather becomes hot again on its completion, the valley freezes once again. On the other hand, if the weather becomes cool after the rainy season, the ice fails to reform. During winter, Ice Valley does not freeze but is instead immersed in fog, while the surrounding area freezes and is covered with snow until April (see Tanaka, 1995).

The mechanism to freeze in the hottest season is not understood well. According to Ohata *et al.* (1994a,b), perennial ice at the Fuji Ice Cave in Japan is formed by the cold dry air inflow into the ice cave during winter, which accumulate cold air into the cave to freeze the cave ice. During summer, on the other hand, the lava tube cave of 150 m length forbids the warm air to come into the cave by the stable stratification. Therefore, the selective convection in winter and summer acts as a thermal filter which allows only coldness to accumulate in the lava tube cave. The Ice Valley's ice is, however, different from the ordinary perennial

ice in cave in that; i) there is no ice in winter, ii) it grows in spring when the outside air temperature is well above the freezing point, and iii) the ice forms in the wind cave near the surface where moss can grow by solar radiation and the temperature outside can be higher than 30°C. Hence, the knowledge for the perennial ice in the lava tube cave does not offer much help in understanding the mystery of the Ice Valley. In particular, the unusual characteristics such that it grows more when temperature is higher in summer are not explained from the theory for ordinary cave ice.

Some theories to explain the Ice Valley's ice have been proposed. Kim (1968) attempted to explain the phenomenon by adiabatic expansion of air blowing through the narrow space of the wind cave. It requires very strong wind blowing at the exit of the wind cave which is in fact not observed. Moon and Hwang (1977) proposed that latent heat absorption by evaporation from capillary zone in the talus cools debris to form ice. Some mechanism is necessary for this theory to cool the dew point temperature which is below the freezing point. Fujiwara (1985) and Bae and Kayane (1986) explains the ice formation by selective convection of cold air during winter as in the lava tube cave ice. For this case, the problem mentioned in i) through iii) remains unsolved. Tanaka (1997) conducted a numerical experiment of Ice Valley's ice based on the selective convection theory. The physical processes considered in the model are buoyancy, Rayleigh friction, adiabatic heating, Newtonian cooling, diffusion of air, and thermal conduction of the talus. The result of the experiment supports the selective convection theory showing cold air penetration deep inside the talus during winter and that the wintertime ice is preserved until the next summer. However, the freezing line with zero degree temperature descends down the under-ground about 50 m depth in summer by the diffusion of the outside hot air. Therefore, the mysterious behavior of the Ice Valley's ice is unsolved.

Recently, it is said that the amount of ice formation during summer is gradually decreasing, probably due to the growing vegetation. Yet, cutting vegetation would not necessarily prevent the decreasing trend because we still do not know how the ice forms during summer. On the contrary, cutting vegetation or any kind of protection effort for ice by the local government might cause further destruction of the summertime ice. That would be a serious problem as the Natural Monument of the Ice Valley as a unique summer resort. Hence, the first step to protect the Ice Valley is to understand the mechanism how the unnatural summertime ice forms. Before conducting further numerical simulations of the Ice Valley, we do need more comprehensive observational studies. For this reason, we have conducted *in situ* observation during June 3 to 5, 1997 as a collaborative study between the University of Tsukuba, Japan and the Pusan National University, Korea. This paper documents the comprehensive observational result for the Ice Valley. Refer to Tanaka *et al.* (1998) for the color pictures of Ice Valley.

2. Description of the Ice Valley

Ice Valley (128° 59' E, 35° 34' N) is located in the upper reaches of the Milyang River (a branch of the Nakdong River) in the northern part of Milyang, Kyungnam, which is in the south-eastern part of the Korean Peninsula (see Fig. 1). It is about 1.5 km north-eastern part of Choun Hwang Mt., 1,189 m high above the sea level. Southern side of Choun Hwang Mt. is a broad plateau with an area of about 4.7 km². Ice Valley is located along the northern slope of the mountain, covering its drainage of about 0.6 km² (see Photo 1). The valley is about 250 m wide and 750 m long with a gradient of 15 ~ 20 degrees. Along the east, west and south sides of Ice Valley there are precipitous terraced cliffs which are several tens of meters high (see Photo 2). The cliffs are made of andesite rocks

and have developed vertical joints. All of the bottom and some parts of the slope of the valley are covered with andesite debris particles which are about 0.5 ~ 2 m in diameter. It is estimated that the depth of debris is about 400 m near the cliff which stands in the upper area of the

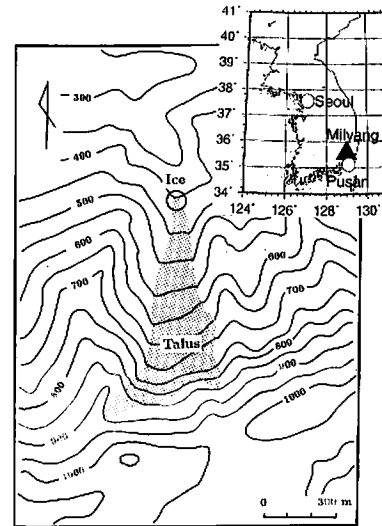


Fig. 1. Location of the Ice Valley in Milyang, Korea. The talus area is shaded. The Ice Valley's ice is located at the bottom of the talus near the 400 m level marked by a circle (after Tanaka, 1997).

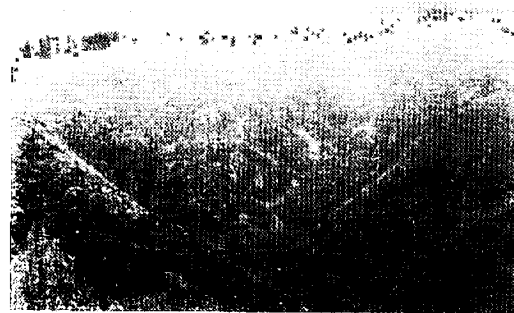


Photo 1. Panorama view of the Ice Valley. The ridge is approximately 1000 m and the bottom of the picture is about 300 m in height. Ice grows around 400 m level which is the bottom of the "V"-shape valley in the photo.



Photo 2. General view of southern cliffs and falling andesite debris with its diameter about 1.5 to 2.0 m.

valley. There are some debris with a smaller diameter made of rhyodacite and tuff.

The freezing area of the Ice Valley is located near 410 m level above the sea level at the very lower end of widely spreading andesite debris as marked by a circle in Fig. 1. A small fence is built at the best freezing area in the eastern slope of the talus to keep tourists out (see Photo 3). The vertical cross section of the valley is presented (speculated) in Fig. 2 in which the location of ice is indicated by a box near 410 m point. Henceforce, the location within the valley is expressed by the altitude from the sea level such as 410 m point along the valley line. In the freezing area, large debris and boulders of about 1.5 ~ 2.0 meter in diameter covers the talus. There are plenty of free spaces between the rocks, so the outside air can penetrate freely into the porous media of talus. Although heat can not be conducted deeper into the talus due to the insulation effect of surface debris, convective motions of air may be possible deep inside the talus. The entire talus is filled with humus soil below the 380 m point. Therefore,



Photo 3. General view of the talus along the eastern slope of Ice Valley. Ice Valley's ice is in the fence to protect from tourists. The plate stands for Ice Valley in Korean letter.

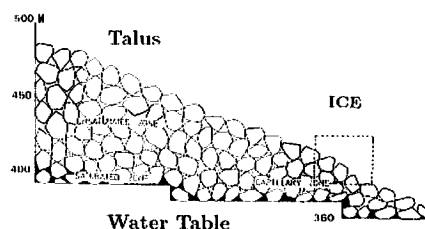


Fig. 2. Cross section of the talus (speculation). The talus consists of large boulders of andesite debris and has water table at the bottom. Unsaturated capillary zone is formed above the water table. The Ice Valley's ice is observed within the square-box area (after Moon and Hwang, 1977).

trees are growing on this soil along the very bottom of the valley. The bottom vegetation extends above the 410 m point along the north-south valley line. Thus, the talus is divided roughly in two branches along western slope and eastern slope separated by the bottom vegetation. Because of the wide coverage of

vegetation, there is no open talus below the 380 m point, and a narrow mountain trail with approximately 2 m width connects the freezing area at 410 m point with shrine and the tourist hotel at the entrance region of the Ice Valley located at 300 m point. Under ground water appears as cool water spring at 360 m point and river stream connects to the Milyang River about 250 m level. Three high water falls hanging on the cliff with no vertical joints are situated in a small valley to the east of Ice Valley. The warm stream of the small valley joins to one from Ice Valley at the entrance of Ice Valley (see Bac and Kayane, 1986).

According to the Milyang Meteorological Observatory, located 25.4 km south-west of Ice Valley, the region has the following climate facts: Precipitation amounts to about 1200 mm per year, being very little during late fall to early spring. In summer before the rainy season, the duration of sunshine and the amount of evaporation are much considerable. In the rainy season, two-third of the annual precipitation falls during this period as local downpours and heavy rainfall. The average relative humidity and the average air temperature for summer are higher than 70% and 27°C, respectively. But in winter, relative humidity decreases to less than 60%, and the average air temperature is below 0°C. The coldest monthly mean temperature is -5°C in February.

Temperature of underground water measured at the spring is about 8°C throughout the year. Ground temperature at the Observatory is about 15°C throughout the year. Therefore, annual mean temperature of this area is well above the freezing point (see Hwang and Moon, 1981).

3. Observation items and method

3.1 Time series of temperature, humidity and radiation

We prepared Micro-loggers provided by Spirig data logger series for temperature (Celsi Pick), humidity (Humi Pick), and light intensity

(Lux Pick). The Spirig data logger is a small data logger about 40 mm by 40 mm by 15 mm size made in Switzerland. The logger can store 2000 data in its memory. Once the logger is set up by PC, it starts to measure 2000 data within the specified time duration. For example, if we set the Celsi Pick for one hour, the logger measures 2000 temperature data within one hour. If we set it for one day, it measures 2000 data within one day. And if we set it for one year, it can measure even annual cycle. The error range for temperature is noted as $\pm 0.2^\circ\text{C}$.

In present observation, we set the temperature Micro-loggers in the wind caves at 300, 350, 410, 450, and 500 m points along the valley line of the eastern talus to measure diurnal variation for June 3 to 5. If there is no wind cave, the logger is put at the narrow open space between rocks similar to the wind cave to avoid direct solar radiation. In addition, we put them at 360, 375W, 380W, 385W, 420W, 435, 450W m points for one day from June 4 to 5. Where, the suffix W denotes western talus, and others denotes eastern talus. Humidity is measured at 300, 410, and 450 m points for June 3 to 5. Lastly, light intensity is measured at 410 m point for June 3 to 5.

In addition to the Spirig data logger series, we prepared the ML data logger series for temperature (ML1751) and humidity (ML1752). The ML data logger series is a Micro-logger of 75 mm by 45 mm by 23 mm size made in Germany. With these ML data loggers temperature and humidity at 410 m point but different depth from the Spirig data loggers are measured. One ML data logger with external sensor was set at 360 m point to measure water temperature.

At the end of the observation, we have left 6 Micro-loggers in the wind caves at various locations and depth in order to measure annual variations of temperature. Unfortunately, all of them were lost when we visited Ice Valley in the next year to pick them up, probably due to flooding by unexpected temporal heavy shower.

One logger was picked up by tourists and

delivered kindly to us. A careful and tight fixing of loggers were needed.

3.2 Vertical sounding of temperature and humidity

The wind cave temperature is close to 0°C while the upper air temperature is around 30°C in the hottest summer. Vertical profiles of air temperature and humidity are the important items to understand. Spirig data loggers for temperature with external sensor and humidity were set for two hours duration with four second interval for the vertical sounding. The set of Micro-loggers were lifted by a balloon and a string (see Photo 4) and sustained for one minute at 10 m interval from 0 m to 100 m range. In addition, the first 10 m range was measured at 1 m interval by the same procedure. The instrument is occupied by a small umbrella to avoid the influence of solar radiation. One measurement of the vertical sounding for a round trip takes approximately one hour. An extensive observation period for one hour is referred to as Run. During the observation, 4 sets of Run

were carried out and are named as

Run-1: 15:00—16:00, June 3

Run-2: 17:00—18:00, June 3

Run-3: 10:00—11:00, June 4

Run-4: 14:00—15:00, June 4

With this method it is possible to measure vertical profiles as high as balloon can lift. Korean group successfully conducts vertical observation up to 200m height. For the successful observation, horizontal wind must be sufficiently weak.

3.3 Observations by AWS

A system of Automatic Weather Station (AWS) was installed at the 410 m point. The system measures time series of temperature, humidity, wind speed, wind direction, and solar radiation at about 1.5 m height from the ground using the instruments seen in Photo 5. The AWS was offered by the group from the Pusan National University.



Photo 4. Vertical sounding of temperature and humidity using Micro-loggers.

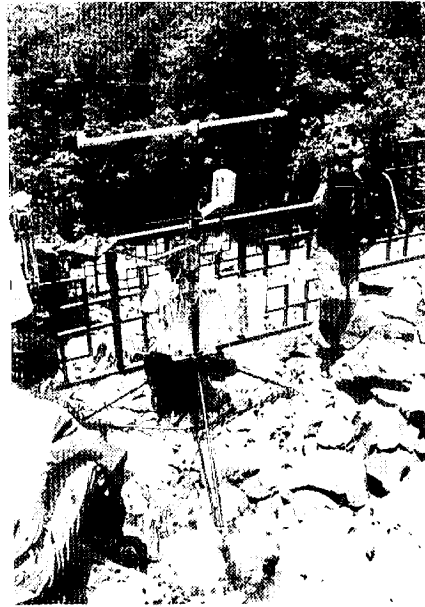


Photo 5. AWS installed at 410 m point near the fence area.

3.4 Moving observations

One of the most important subjects of present observation was to identify the location of air intake to the inside talus to compensate the outflow of cold air from the wind caves. The theory of mass continuity requires that there must be air intake somewhere on the talus as long as cold air keeps blowing from the freezing area. Teams of moving observations climbed the talus from the bottom of 300 m point to the top of 780 m point. Many tiny caves are measured with digital thermometer-anemometer and burning incenses to check whether the cave shows outflow or inflow. Surface air temperature, humidity, and wind are recorded over the wider area of the Ice Valley.

3.5 Other observations

(a) Air temperature, dew point, and wind were observed by Assman ventilated psychrometer and rotation anemometer at 350, 410, and 450 m point. Basic information of cold air drainage is obtained by them.

(b) Thermograph was used to see skin temperature over the talus. It is hard to convince the overall situation of Ice Valley indicating 0°C at the wind cave under a boulder while the upper surface of the same boulder is heated well above 30°C by solar radiation. Thermograph offers the temperature distribution from 0°C to 30°C in a single picture.

(c) Fiber Scope CCD camera was used to view deep inside the wind cave (see Photo 6). It is important to answer whether there is ice deep inside the cave or ice is confined only at the wind cave exit area. Although we cannot see very deep part of talus, the Fiber Scope offers some answer about the interior of the wind cave.

(d) An freezing experiment was conducted by putting a cup of water beside big ice in the wind cave to see if it freezes or not. If temperature is cold enough to freeze water in the cup, we can predict that ice would grow as far as water is supplied by precipitation. The



Photo 6. Fiber Scope CCD camera to see deep inside the wind cave.

amount of ice is therefore controlled by the water supply from rain.

(e) We brought small pieces of rocks back to Japan to analyze the type, measure density, and measure specific heat. Many photo and video were taken to explain the Ice Valley's mysterious ice.

4. Result of observation

4.1 Ice Valley's ice

The observation was carried out from the afternoon of June 3 to the morning of June 5, 1997. Seven graduate students from Japan and five graduate students from Korea joined together to conduct the observation. Weather was fine with a lot of sunshine throughout the period. A cold front passed on June 2 just before the observation. A short evening shower occurred in the evening of June 5. Thus, it was a perfect weather for observation with no rainfall and mild wind during the observation period.

Photo 7 shows general view of the talus

along the western slope. Sedimentation consists of large boulders and debris with 1.5 to 2.0 m in diameter. There is no vegetation along the talus except along the very bottom of the valley.

Photo 8 presents composite pictures of Thermograph along the western slope of the talus corresponding to the Photo 7, showing the skin temperature distribution. The top-most darkest area denotes clear sky. The gray area below it indicates vegetation near the summit. The white area indicates that the rock surface temperature is above 30°C. Between the hot rocks there are a number of cold spots. The bottom picture presents temperature distribution of the wind cave between large rocks. The dark area shows that the wind cave temperature is 0°C.

Photo 9 is an example of Ice Valley's ice in the wind cave growing 20 cm long from the bottom to top. It is not clear how the ice column grows. A speculation is that it grows from the bottom to top like a stalagmite by freezing rainfall water supplied from above as water droplets. Another speculation is that a big icicle grows from the top to bottom to create a ice column. Then the upper part of icicle melts because the air is relatively warmer at the top.

There are icicles as shown in Photo 10 along



Photo 7. General view of the talus along the western slope. Sedimentation consists of large boulders and debris with 1.5 to 2.0 m in diameter. Ice grows in the space between the rocks. There is no vegetation along the talus except along the very bottom of the valley.

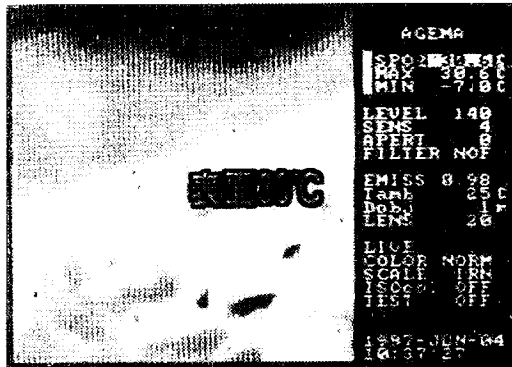


Photo 8. Composite pictures of Thermograph along the western slope of the talus corresponding to the Photo 7, showing the skin temperature distribution. The top-most dark area denotes clear sky. The area below it indicates vegetation near the summit. The white area shows the rock surface with temperature above 30°C. Between the rocks there are a number of cold spots. The bottom picture presents temperature distribution of the wind cave. The dark area means that the wind cave temperature is 0°C.

the vertical wall of a rock surface. It seems that the ice freezes at the cave entrance area, and it melts in the deeper area. There are various kinds of ice other than ice columns and icicles.

Photo 11 shows scattered ice along a gap in the wind cave. There are many small piece ice about 5 cm length. The instrument in the photo is the electric thermometer.

Photo 12 shows white ice containing plenty of air bubble in it. It looks like the remaining snow, but the ice surface is rather clean for this

season. The size is approximately 30 cm length. The white ice is located on the ground without shelter exposed to sky under downward radiation and rainfall, although solar radiation does not reach it directly. Photo 13 shows another example of icicle within the fence area at the 1.2 m depth. The ice spreads over the flat floor and create a large slab of ice. We put Micro-loggers on the ice slab. As an experiment we put a cup of water on the ice slab of Photo 13 for one night. As seen in Photo 14 the result indicates that water is not frozen. Therefore, temperature is close to zero, but not cold enough to freeze fresh water.



Photo 9. Ice in the wind cave growing 20 cm long from bottom to top.



Photo 10. Icicle in the wind cave growing along the rock surface.



Photo 11. Scattered Ice in the wind cave and the electric thermometer.



Photo 12. White Ice in the wind cave which looks like the remaining snow. Snow skin is clean without accumulation of soil and dust. White ice is exposed to the sky.

4.2 Diurnal variations

Figure 3 plots diurnal variation of illumination intensity measured by the Micro-logger at 410 m point. We set the Micro-logger for illuminance observation as soon as we arrived at Ice Valley on June 3. The weather condition was fine from the afternoon of June 3 till the morning of June 5 with occasional shadow by cumulus clouds. The peak intensity is 3.8 lm m^{-2} . The unit lumen measures a brightness in candela. The sunrise is approximately 5:00 and sunset is close to 20:00. We note that the instrument was in tree shadow during the morning. The same diurnal variation of solar radiation measured by the AWS at 410 m point is plotted in Fig. 4 to compare the two different



Photo 13. Ice in the wind cave and micro-logger of temperature and humidity.



Photo 14. A cup of fresh water after one night placed beside the ice slab in the wind cave.

systems. The AWS is located few meters apart from the Micro-logger where no morning tree shadow influences the result. The peak radiation is about 900 W m^{-2} . It decreases in the afternoon of June 4 due to the cumulus clouds. It is interesting to note that the brightness is high after the sunrise and before the sunset. Yet, the amount of energy arriving at the unit area is low compared with its peak values at noon.

Figure 5 plots surface air temperature under

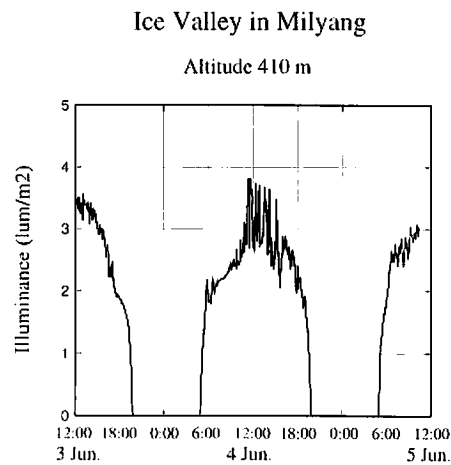


Fig. 3. Diurnal variation of illuminance at the 410 m point during June 3 to 5, 1997, observed by Micro-logger (Lux Pick). Units are lm m^{-2} .

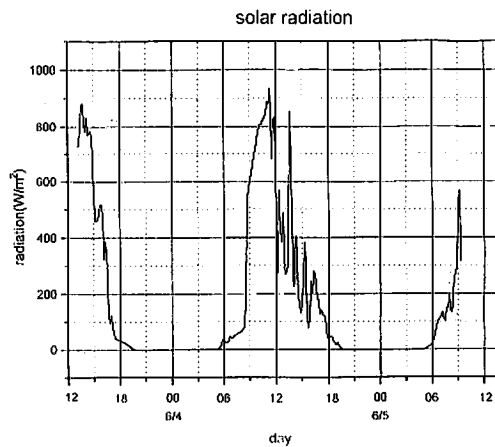


Fig. 4. Same as Fig. 3, but observed by AWS at the 410 m. Units are W m^{-2} .

rocks at 300, 350, and 410 m points from June 3 to June 5. Those three points represent the lower part of the Ice Valley. The 300 m point is located at the bottom of the valley along the river and is regarded as open area without the influence of cold air drainage from Ice Valley. The temperature shows clear diurnal variation within the range from 14°C during night to 23°C during daytime. The 350 m point is close to the spring above which the river water becomes underground water under the talus. The temperature indicates weak diurnal variation between 12°C and 14°C. It is evidently cooler than the 300 m point during the daytime. Cold air flow from wind caves is accumulated in this area. The 410 m point is the location of the fence with major wind cave (see Photo 13). Large ice is formed at several locations in the caves. Cold air of 0°C keeps blowing from the wind cave. The temperature is maintained at the freezing point, and no diurnal variation is detectable.

Figure 6 is a continuation of Fig. 5 but for the upper part of the Ice Valley at 410, 450, and 500 m points. The same curve of 410 m point in Fig. 5 is plotted for convenience. The 450 m point is located at the middle of the exposed debris along the talus slope. The temperature is

approximately constant about 7°C. It is interesting to note that the diurnal variation is absent here although the temperature is well above the freezing point. The 500 m point is close to the top of the exposed debris connected with the wind caves near 410 m point. The temperature varies between 15°C and 20°C. The maximum temperature is lower than that of 300 m point and the minimum temperature is higher than that.

Figure 7 collects other temperature time series for one day period. Locations 360 and 360a illustrate temperature time series at 360 m point in the wind cave and 1.5 m above the ground, respectively. The data 360a indicates clear diurnal variation whereas 360 indicates basically no diurnal variation although temperature itself is well above the freezing point. The result implies that cool air about 8°C keeps flowing from the wind cave near the water spring area. The air temperature coincides with water temperature. The 380 and 385 m points are in the western half of the talus. At 380 m point, the blowing air is 0°C which is the coolest point. Only 5 m above this area at 385 m point indicates considerably warmer temperature.

Figure 8 plots the diurnal variation of humidity at the 300 m point for June 3 to 5. Humidity

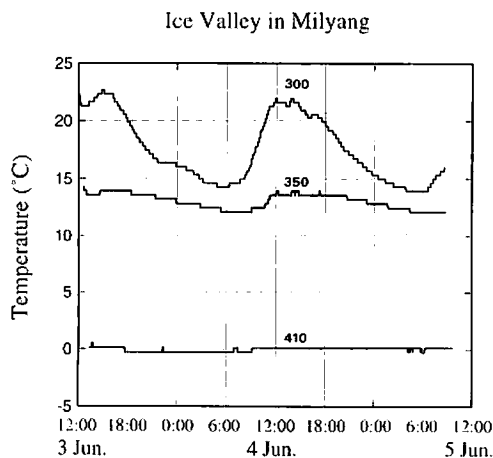


Fig. 5. Diurnal variation of surface air temperature at the 300, 350, and 410 m points.

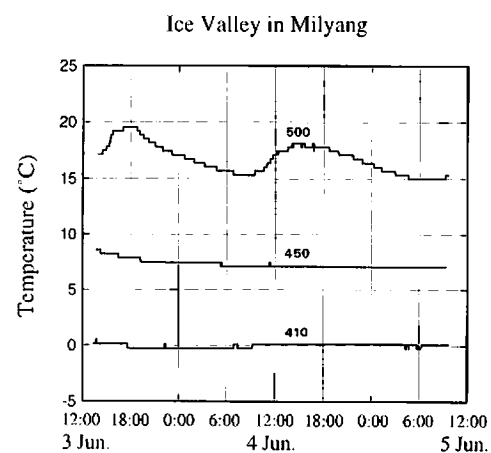


Fig. 6. Diurnal variation of surface air temperature at the 410, 450, and 500 m points.

decreases sharply as temperature increases after the sunrise. The daytime humidity is about 50% at noon, and it increases gradually up to 80% by the sunrise of the next day. Figures 9 and 10 plots the diurnal variations of temperature and humidity at the 1.2 m depth in the wind cave at the 410 m point measured by the ML data loggers (see photo 13). Temperature is kept

constant at about 0.5°C and no diurnal variation is detected. Humidity is kept constant at about 96% and no diurnal variation is seen. It seems that the temperature is slightly warmer than freezing point, and humidity is slightly drier than 100%.

Figure 11 plots the diurnal variation of air temperature and humidity at 1.5 m above the ground by the AWS at the 410 m point.

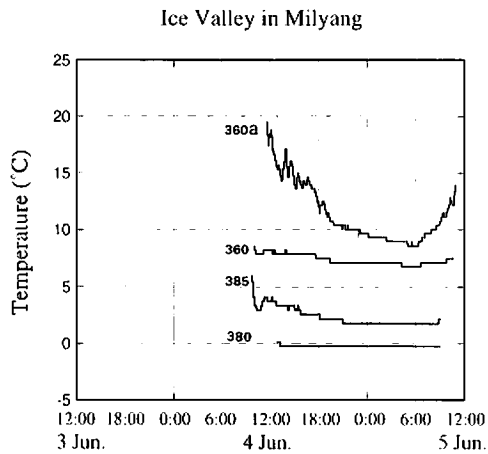


Fig. 7. Diurnal variation of surface air temperature at the 360, 380, and 385 m points. The 1.5 m height temperature at 360 m point is marked by 360a. The 380 and 385 m points are located along the western slope of the talus.

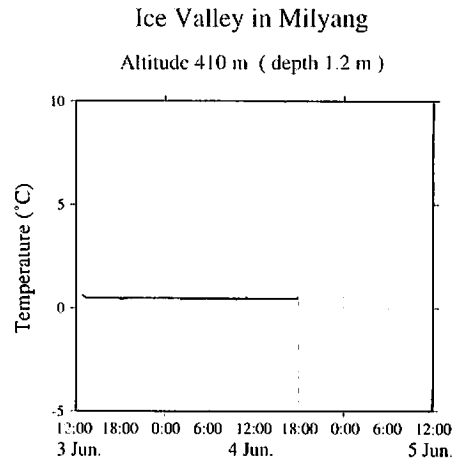


Fig. 9. Diurnal variation of temperature at the 1.2 m depth of the wind cave at the 410 m points measured by Micrologger (ML1751).

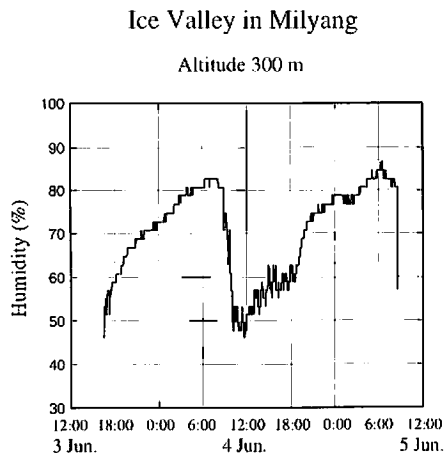


Fig. 8. Diurnal variation of humidity at the 300 m points measured by Micrologger (Humi Pick).

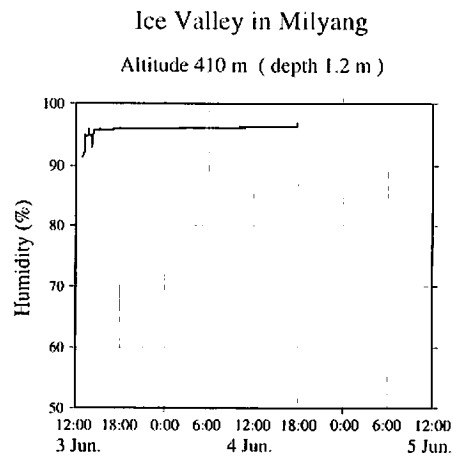


Fig. 10. Diurnal variation of humidity at the 1.2 m depth of the wind cave at the 410 m points measured by Micrologger (ML1752).

Maximum temperature reaches 23°C on June 3, and it is 20°C on June 4. That of June 3 is 3°C lower than previous day, probably due to the increased mixing with cold air from the wind cave. Maximum temperature occurs around 15:00 on June 3, but it is about noon on June 4. The short period variation during the daytime of June 3 may reflect shadow of cumulus clouds. A part of the variation can be influenced by the occasional blow of cold air from the wind cave. The diurnal variation is quite similar to that of 300 m point, although 410 m point indicates slightly lower temperature than that of 300 m point. Minimum tem-

perature is 13°C for both morning on June 4 and 5. Compared with minimum temperature at 300 m point, the value is 1°C lower suggesting the effect of adiabatic lapse rate between 300 and 410 m. Compared with Figs. 9 and 10 at the same 410 m point, the result shows that the sharp temperature gradient is concentrated within the thin layer between 1.5 m and 0 m height above the ground.

Figure 12 plots the wind speed and direction by AWS at 410 m point. Wind direction is consistently south, implying down slope flow of the cold air. The direction is quite steady during night, but it varies much for the daytime. Wind

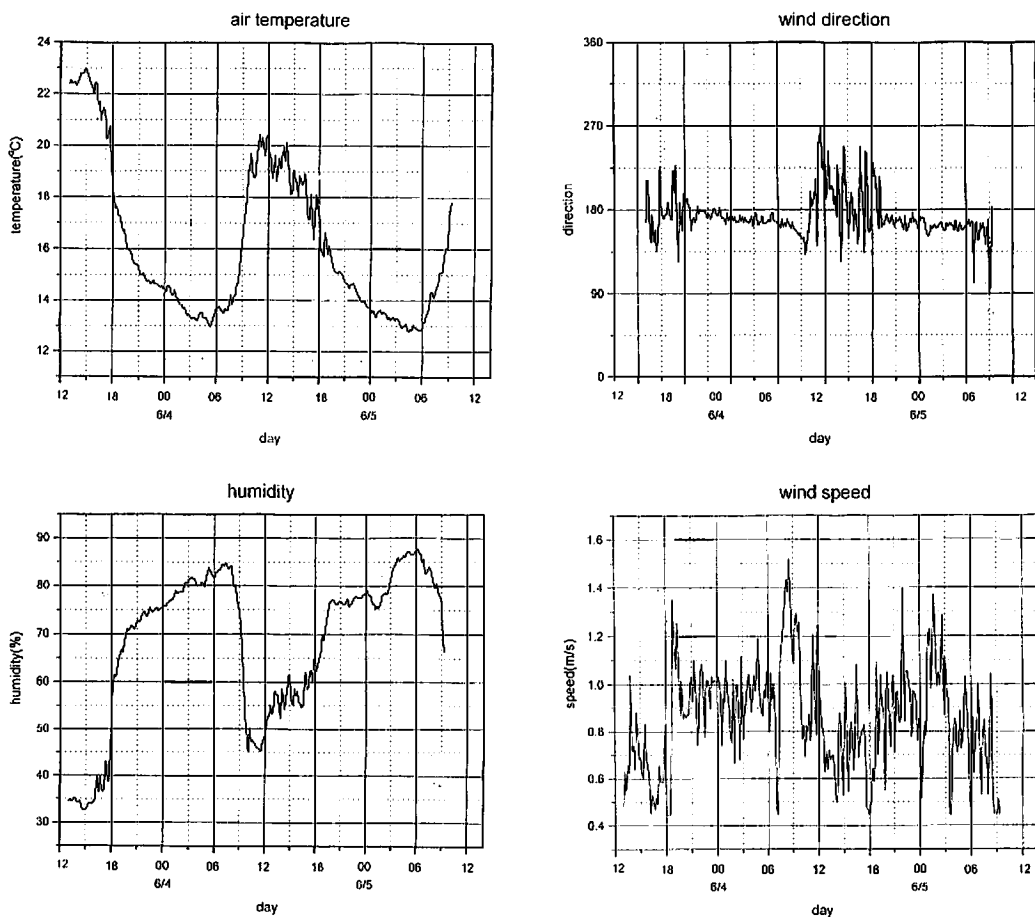


Fig. 11. Diurnal variation of air temperature and humidity by the AWS at the 410 m points.

Fig. 12. Diurnal variation of wind speed and direction by the AWS at the 410 m points.

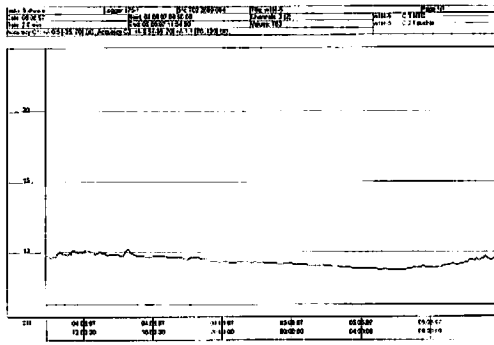


Fig. 13. Diurnal variation of water temperature at the water spring near 360m points.

speed varies from 0.5 ms^{-1} to 1.5 ms^{-1} . When the cold air drains steadily during night, the wind speed is about 1 ms^{-1} for the night of June 3. The dominant time scale of the fluctuation is approximately 40 min. There is a blow of 1.5 ms^{-1} at 09:00, June 4 from the southeast.

Figure 13 plots water temperature at the water spring near 360 m point. The water temperature is about 10°C at noon of June 4 and it

decreases to 8°C in the morning of June 5. The water temperature is very closed to the surface air temperature in the cave shown in Fig. 7 for 360 m point.

4.3 Vertical profiles

Figures 14 to 17 illustrate vertical profiles of temperature and humidity for 15:00, June 3 (Run-1), 17:00, June 3 (Run-2), 10:00, June 4 (Run-3), and 14:00, June 4 (Run-4), respectively. For Run-1, temperature starts from 24°C at the lowest level because the sounding start from about 1m height. Temperature is almost constant for all vertical level up to 100 m. Since the cave temperature is 0°C , enormous temperature gradient is concentrated in the bottom layer about 1 m thick. The same is true for humidity. It is approximately 24% at 100 m level and decreases to 20% at the lower layer. The value increases sharply to 30% at the bottom layer. Since the cave humidity is about 100%, the curve should be connected to the higher values. For this reason, we started the vertical sounding

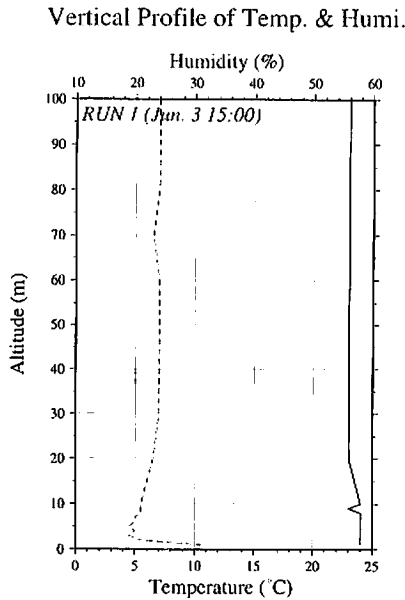


Fig. 14. Vertical profile of temperature and humidity for the Run-1 (14:00, June 3) over the 410 m points.

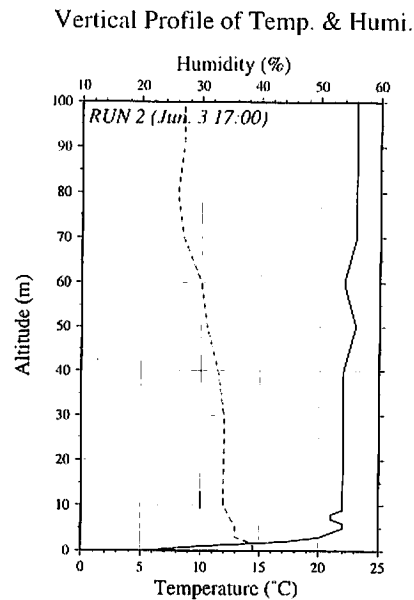


Fig. 15. Same as Fig. 8 but for the Run-2 (17:00, June 3).

from the level 0 m at the outlet of cold cave air for the Run-2 to Run-4.

For the Run-2 at 17:00 the upper air temperature is 22°C that is 1°C lower than Run-1. It decreases sharply at the layer below 5 m level from 22°C to 5°C at the 0 m level. Humidity changes from 23% to 40%. For the Run-3 at 10:00 temperature is 22°C at 100 m level and 24°C at 5 m level. It decreases to 5°C at 0 m level. Humidity varies from 23% at 100 m to 15% at 10m level. It increases to 40% at 0 m level. Finally, for the Run-4 at 14:00 temperature is 21°C at 100 m level, 24°C at 20 m level, and 21°C at 4 m level. It drops to 3°C at 0 m. Humidity is 43% at 100m and a dry layer is seen around 20 m. It returns to 50% at 0 m level.

Compared with the time series of AWS at 410 m point in Fig. 11, we can assess the result by AWS as a very sensitive one depending on the thickness of the cold air drainage. The observed values would change drastically if we move the instrument even a half meter in the vertical. For example, the upper air temperature is 24°C at 14:00 whereas the AWS temperature

decreases from 20°C at 10:00 to 16°C at 18:00. Part of the temperature decrease may be related to the expansion of cold layer during the daytime. Humidity increases markedly at 18:00, June 3. It coincides with decreasing temperature and with increasing katabatic wind speed. Next morning, humidity decreased abruptly at 09:00 which coincides with increasing temperature and the abrupt blow of wind from southeast.

4.4 Cross sections

By the vertical sounding using helium balloon, we can observe not only temperature and humidity but also wind direction. The down-slope wind of about 1 ms⁻¹ near the surface is rather shallow. When the balloon lifts above the katabatic wind layer, we observed that the balloon tilts opposite direction toward the summit. Namely, above the thin layer of katabatic wind, there is a valley wind from valley to the summit as for the ordinary mountainous region during the daytime. According to our moving observation over the talus, we found that the katabatic wind of cold

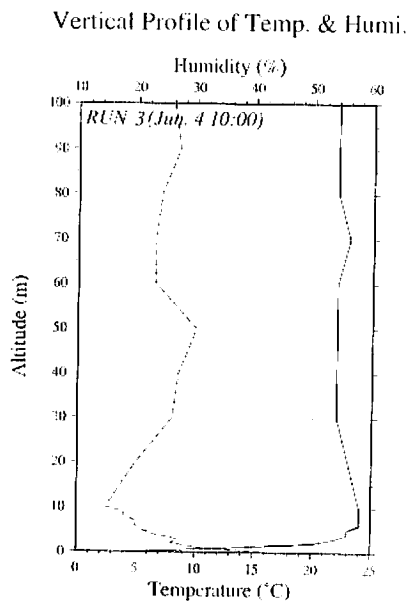


Fig. 16. Same as Fig. 8 but for the Run-3 (10:00 June 4).

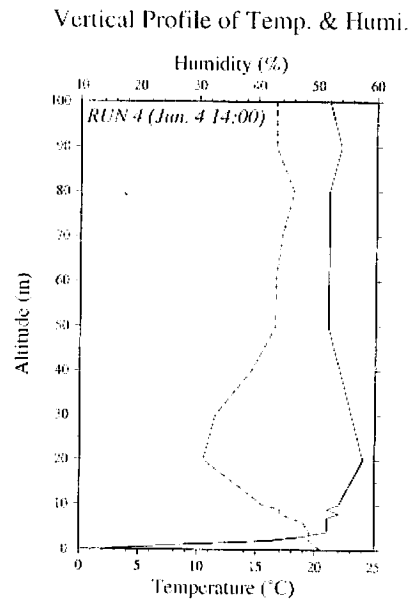


Fig. 17. Same as Fig. 8 but for the Run-4 (14:00 June 4).

air gradually evanescent as we move up. The katabatic wind is replaced by the anabatic wind at 430 m level: only 20 m above the fence area. The result is consistent with our vertical sounding with balloon.

Figure 18 illustrates a schematic cross section of wind vectors and temperature distribution over the talus. The corresponding plane diagram of wind vectors and temperature distribution is presented in Fig. 19. The surface air is the coldest at the 410 m point. Temperature increases both in the upper and lower area apart from the 410 m point. We found that diurnal variation is missing in the time series data as long as wind blows from the wind cave even though cave temperature increases well above the freezing point. The katabatic wind begins at 430 m point where the cave temperature is about 10°C. The cold air from the wind cave merges and accumulates to 5 m thick at 410 m point. The flow is strongest at the 380 m point converging in the narrow path surrounded by tall vegetation at the valley. The cold air from wind cave continues to blow at the 360 m point near the water spring indicating the

cave temperature about 8°C. Above this cold air layer, there is an ordinary valley wind from valley to the summit with air temperature 24°C. The result suggests that the cold air drainage near the surface and the warm upper air valley

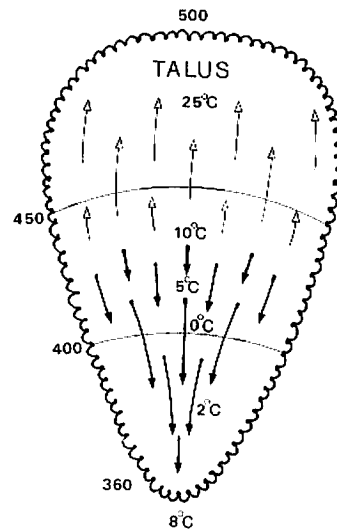


Fig. 19. Spatial distribution of the flow pattern over the talus for the Run-4 (14:00 June 4).

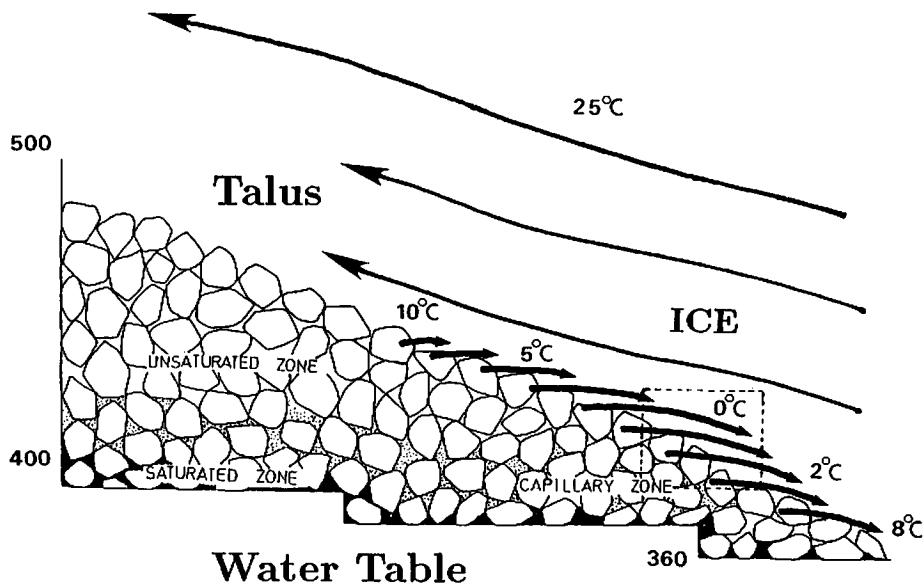


Fig. 18. Schematic illustration of the cross section of the air flow pattern along the Ice Valley for the Run-4 (14:00 June 4).

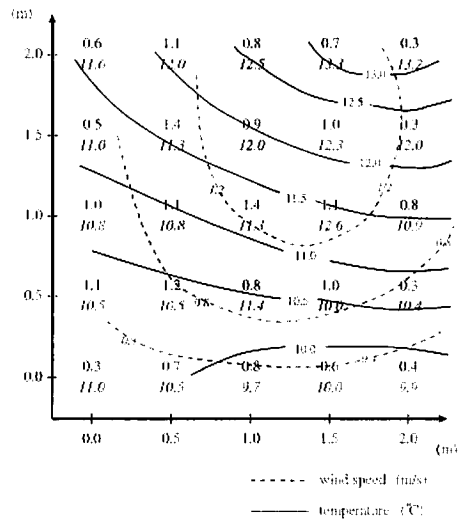


Fig. 20. Vertical cross section of temperature and wind speed for the narrow mountain trail along the valley near 380 m point for the Run-4 (14:00 June 4).

wind are different wind system. It is unlikely to consider the warm upper air being cool down by contacting with cold debris to create the cold air drainage as discussed by Tanaka (1997) in a closed domain model simulation.

Figure 20 illustrates temperature and wind cross sections perpendicular to the trail at the 380 m point. The trail has approximately 2 m width surrounded by tall vegetation more than 10 m height. The strongest wind core is located at 1.5 m height showing the wind speed of 1.5 ms^{-1} . Temperature is 10°C at the bottom and 13°C at 2 m height. We can roughly estimate the mass flow as $4 \text{ m}^3\text{s}^{-1}$ along the trail.

5. Summary and discussion

The Ice Valley's ice appears during spring to summer and it disappears during fall to winter. It has been said that the hotter the summer is, the more the summertime ice grows. Despite this intriguing nature, the mechanism to freeze in the hottest season is not understood well. Recently, the amount of ice formation is said to

be gradually decreasing, probably due to the growing vegetation. Yet, cutting vegetation would not necessarily prevent the decreasing trend because we still do not know how the ice forms during summer. On the contrary, cutting vegetation or any kind of protection effort might end up with destruction of the summertime ice. That would be a serious problem as the Natural Monument of the Ice Valley as a unique summer resort. The first step to protect Ice Valley is to understand the mechanism how the unnatural summertime ice forms. For this reason, we have conducted *in situ* observation during June 3 to 5, 1997 as a collaborative study between the University of Tsukuba, Japan and the Pusan National University, Korea.

As a result of the *in situ* observation, following facts are found:

1. The vertical sounding at 410 m point shows in average that the upper air temperature beyond 5 m height is 24°C and humidity 25%. Within the layer 5 m above the ground, the temperature decreases rapidly from 24°C to 0°C at the ice location in the wind cave. The temperature gradient is especially large below 1 m height. Likewise, the humidity increases from 25% to 100% within the thin layer.
2. Air temperature from wind caves is 0°C at the freezing area from 380 to 410 m points. It warms up to 10°C at 430 m in the upper region and 360 m in the lower region. We find that there is no diurnal variation in temperature where cold air blows out from wind cave for the region from 360 to 430 m points.
3. Cold air blowing from the wind cave at the freezing area merges to produce cold air drainage (katabatic wind) of 1 ms^{-1} at the narrow trail. The cold air drainage at 410 m points is confined within 5 m height. Above 5 m height, ordinary valley wind (anabatic wind) is observed. The surface cold air drainage is observed up to 430 m point. Beyond this altitude ordinary valley wind

with 24°C takes over even at the surface.

The result suggests that the cold air drainage below and valley wind above are separated wind system with no continuity. According to the numerical simulation of Ice Valley by Tanaka (1997), a marked cold air flow is induced over the surface by the cooling of surface air by cold talus. The cold air flow for such a closed mass system is compensated by a counter flow well above the valley. A circulation predicted by such a closed domain model appears to be misleading. The contradiction of the model result found by present observation suggests that the numerical modeling of Ice Valley must be formulated in an open domain, allowing general valley wind of typical mountainous region.

It is found that the diurnal variation of temperature is a good indicator to identify the wind cave. When a cave is filled by soil and no air is coming out, the cave feels diurnal variation; thus the cave is not a wind cave. Even if the temperature is well above the freezing point, constant temperature is maintained as long as air comes from deep inside the talus; thus the cave is a wind cave. According to this recognition, the wind cave at Ice Valley is distributed over the region from 360 to 430 m point. Since 360 m point is the location of water spring, air coming out from the wind cave must be compensated at the region above 430 m point. It is often the case that a wind cave is accompanied by a warm wind cave which blows warm air during winter. According to the report by Egawa *et al.* (1980) and Yokoi (1999) the warm wind cave is located about 100 m above the ordinary cold wind cave. When the warm wind cave blows warm air during winter, it may be quite reasonable to speculate that the blowing warm air is compensated by an intake of winter air from the location of the cold wind cave 100 m below. On the contrary, we can safely speculate that the cold air blowing from the wind cave is coming from the inflow from the warm wind

cave 100 m above during summer. Although the location of such a warm wind cave was not identified by present observation, we can speculate that the air is compensated at the region above 430 m point and below the cliff.

If this is the case, the result of present observation supports the selective convection theory in winter and summer for the mechanism of ice formation. According to Bae and Kayane, there is no snow over the talus during winter despite that surrounding area has accumulated snow. This is a clear indication that a wide area of Ice Valley is the warm wind cave. Further studies are necessary to identify the extension of warm wind cave in terms of winter observation.

Acknowledgments

The authors are grateful to Mr. Y. Sugiyama, Director of Fuji TV, and Mr. T. Iwaya, Certificated Weather Forecaster of Japan Weather Association for their cooperation of the observation. The appreciations are also due to the assistance of seven graduate students from University of Tsukuba, Japan and five graduate students from Pusan National University, Korea. The first author acknowledges Ms. Honda for her technical assistance.

References

- Bae, S.K. and Kayane, I. (1986): Hydrological study of Ice Valley, Korea. *Ann. Rep., Inst. Geosci., Univ. Tsukuba*, **12**, 15-20.
- Egawa, Y., S. Hori, and T. Sakayama, (1980): On the origin of wind cave. *J. Geology*, **89**(2), 1-12 (*In Japanese*).
- Fujiwara, S. (1985): Wind cave at Souunzan in Hakone. *Kisyo*, **29**, 5, 8135-8137 (*In Japanese*).
- Hwang, S.-J. and Moon, S.-E. (1981): On the summertime ice formation at Ice Valley in Milyang, Korea. *Abstracts in Spring Conference, Geophysical Soc. Japan*, **19**, 218-219 (*In Japanese*).

- Kim, S.S. (1968): On the ice formation at the Ice-Valley, Milyang Koon, Korea in summer season. *J. Korean Meteor. Soc.*, **4**, 13-18 (in Korean with English abstract).
- Moon, S.-E., and Hwang, S.-J. (1977): On the reason of the ice-formation at the Ice-Valley, Milyang Kun, Korea in the summer season. *Pusan National University. Paper collections*, **4**, 47-57 (in Korean with English abstract).
- Ohata, T., Furukawa, T. and Higuchi, K. (1994a): Glacioclimatological study of perennial ice in the Fuji Ice Cave, Japan. Part 1. Seasonal variation and mechanism of maintenance. *Arctic and Alpine Research*, **26**, 227-237.
- Ohata, T., Furukawa, T. and Osada, K. (1994b): Glacioclimatological study of perennial ice in the Fuji Ice Cave, Japan. Part 2. Interannual variation and relation to climate. *Arctic and Alpine Research*, **26**, 238-244.
- Tanaka, H.L. (1995): Mysterious ice valley in Korea where ice grows during the hottest season. *Tenki*, **42**, 647-649 (In Japanese).
- Tanaka, H.L. (1997): A numerical simulation of summertime ice formation in the Ice Valley in Milyang, Korea. *Geogr. Rev. of Japan*, **70A**-1, 1-14.
- Tanaka, H.L., Moon, S.-E., and Hwang, S.-J. (1998): Mysterious Ice Valley in Korea where ice grows during the hottest season. *Tenki*, **45**, 825-826 (In Japanese).
- Yokoi, M. (1999): Observational and theoretical studies on the cause of the cold air flow from wind caves at Nakayama in Shimogo Hukushima. *Graduation Thesis, College of Natural Sciences, University of Tsukuba (In Japanese)*.
-

